Chapter 13
Robust Optimal Multi-agent-Based Distributed Control Scheme for Distributed Energy Storage System

Desh Deepak Sharma and Jeremy Lin

13.1 Introduction

Worldwide, there is a rapid growth of renewable power generations, especially wind and solar PV, which have made inroads into the existing electricity grids. According to the International Energy Agency Photovoltaic Power Systems Programme (IEA-PVPS), this growth rate in installed capacity is ranging from 35% to 85% in Organisation for Economic Co-operation and Development (OECD) countries. The IEA-PVPS has shown that 40 GW of solar capacity has already been installed around the world. The energy from installed solar PV would increase to 600 GW in 2035 due to decrease in expenses and government aids. In 2035, the expected solar capacity would reach 113 GW in China, 85 GW in India, and 54 GW in Japan [1].

Furthermore, IEA-PVPS has analyzed that hybrid PV system configuration such as PV and BESS are economical and clean [2]. The hybrid PV system is basically a microgrid in which DC link can be shared between PV system and BESS [3]. During recent years, installed price of solar PV system has decreased due to decrement in the hardware cost. Expected financial returns and concerns about operations and maintenance are the major other determining factors in the adoption of solar PV system [4]. The storage systems paired with solar plants can overcome the risks, faced by the solar power producer, due to uncertain production of solar plant [5]. The variability and uncertainty feature in solar PV power and wind power generation must be analyzed in order to develop a mechanism for evaluating both the economic and

D. D. Sharma (✉)
Electrical Engineering Department, M.J.P. Rohilkhand University, Bareilly, India
e-mail: ddsharma@mjpru.ac.in

J. Lin
Transmission Analytics, Austin, TX, USA
e-mail: Jeremylin@transmissionanalytics.net

B. Mohammadi-ivatloo, M. Nazari-Heris (eds.), *Robust Optimal Planning and Operation of Electrical Energy Systems*,
https://doi.org/10.1007/978-3-030-04296-7_13

reliability impacts of solar PV and wind power variability and uncertainty at multiple scales [6].

Possibilities of uncertainty in forecasting may be due to different factors. In various literatures, different models are developed for forecasting, but these methods are based on a number of assumptions of the future. Forecasting may not be accurate due to collection of bad input data found from either measurement or estimation. It is impossible to perfectly develop the relationships among all possible factors and output of a system. Reliability and security will be the new challenges in the development of a smart grid with the penetration of more and more renewable sources which are uncertain in nature in terms of power generation. In the presence of uncertainties, the grid can be made more secure and reliable by deploying energy storage devices as new technology in the system. With both grid-connected and islanded operations, intelligent energy management schemes are developed while deciding the capacity and charging rate of storage devices, residential load variations, and distribution network electricity price [7, 8].

A solar photovoltaic (PV) unit consists of a number of solar cells. In solar power generation of each cell, modeling has been done for two parts such as the solar irradiation function and the power generation function in which solar irradiation is linked to the power output of the solar PV generator. In different literatures, it is found that, generally, the beta PDF is being used in the modeling of the random behavior of the solar irradiation for each day. The parameters beta PDF can be inferred from the estimates of mean and variance values of historical irradiance data [9–11]. Based on the model of irradiation distribution, the output of a solar generator is decided by the function of power generation [12]. Similarly, in wind turbine generation modeling, two parts are considered as wind speed modeling and the turbine generation function. For modeling of wind speed randomness, the Weibull distribution is generally used. Forecast values and associated uncertainties of wind power are important to the utilities. These information help in optimal scheduling of energy storage and distributed generations [13]. At substations, load patterns are uncertain as compared to that at large system. Several qualitative and quantitative variables influence the electrical load demand. Some of these variables are random in nature, and, hence, the load demand is uncertain. The shape of curve representing the typical load pattern can be expressed in a group of deterministic variables which show the qualitative characteristic of the load pattern. Some groups of load patterns may be based on weekdays, weekends, or holidays. Others may consider the seasons such as autumn, winter, spring, and summer [14, 15]. A new empirical method is developed to model the prediction uncertainty of the solar irradiance forecast on numerical weather prediction. The predicted and measured solar irradiances are transformed into Gaussian random variables with past observed data, and a multivariate normal joint distribution model is estimated using this data [16]. A periodic optimization method is developed that determines an optimum periodic solution for any load profile over a 24-h period. The cyclic solution for the battery state of charge is represented by Fourier coefficients. The optimization process is embedded in a receding horizon battery control system [17].

In smart grid infrastructure, the distributed multi-step optimal scheduling is introduced for energy storage devices and distributed generation. This algorithm is

based on the local communications with neighbors [18]. In order to reduce generation cost, in microgrid, the distributed optimal strategy is proposed for the resource management [19]. The computationally tractable distributed optimal control strategy, which includes AC optimal power flow, for batteries is proposed in a microgrid [20]. Multi-agent-based optimal distributed charging rate scheme is proposed for numerous plug-in electric vehicle (PEV). In this scheme, an agent for a PEV decides optimal charging rate based on remaining charging time and state of charge along with other battery parameters [21]. In smart grid, an adjustment cost is considered for dynamic adjustment of distributed generations and loads. In distributed control algorithm, this cost is minimized to achieve generation-demand balance [22]. A multi-agent-based dynamic optimal power flow is suggested for microgrid with energy storage devices and distributed generations [23].

13.2 Multi-agent System

A multi-agent system is a group of interacting agents that acts in a concurrent way existing in the distributed environment. They have cooperation as well as competition among themselves, and they are conjunct in some common infrastructure. In MAS local goals of individual agents are more important to be accomplished as compared to the overall system goal [24–28].

13.2.1 MAS for Power System: An Overview

The penetration of various distributed generations into the electric network and liberalization of electricity markets with new business models pose the new challenges to the power industries such as enhancement of complexity in distribution network, problems in power system management, disturbance of power system protection, and frequency stability [26, 29]. Present power system equipped with old legacy SCADA system does not suffice to cater aforementioned challenges in highly decentralized system [26, 30]. Market-based MAS is proposed in [31] for reconfiguration of radial shipboard power system, developed with Java Agent Development Framework (JADE) which conforms to FIPA standards for intelligent agents. MASCEM, a multi-agent simulator system, is a framework which deals with new rules, new behavior, and also new actors involved in various electricity markets within liberalized and competitive environment [32]. ABMS, agent-based modeling and simulation system, based on traditional game theory, is able to perceive and analyze the complexities of power market (e.g., repeated auctions, fluctuating supply and demand, non-storability of electricity, etc.) and interactions among all entities involved [33]. In multi-agent approach to power system, each bus agent (BAG), which possesses local information, tends to restore load after fault occurrence, directly connected to its associated bus interacting with other numerous BAGs,

and a single facilitator agent (FAG) acts as a manager for the negotiation process [34].

Multi-agent system is developed for monitoring of transformer condition [35] and industrial gas turbine start-up sequence [36]. An agent-based automation system is developed for substation, while the information is gathered by control/monitoring agents over Ethernet network [37]. A multi-agent system is also capable in efficient operation of microgrids with minimum operation cost [24, 38]. PEDA (Protection Engineering Diagnostic Agents), a multi-agent system, which complies FIPA standards, integrates legacy intelligent systems SCADA and digital fault recorder data and can interpret intelligently and manage data online [30, 39]. As virtual power plant (VPP) is scattered in a decentralized system, multi-agent system facilitates virtual power point to take decisions at local level so that the main goal is achieved [24, 25].

13.2.2 Preliminaries

Let $V = \{1,\ldots,n\}$ be a set of nodes and $E \subseteq V \times V$ be a set of edges of a weighted digraph (or directed graph) $G = \{V,E,A\}$. $\boldsymbol{A} = [a_{ij}]$ be the adjacency matrix with non-negative adjacency elements a_{ij} and $a_{ii} = 0$ for $i = 1, 2, \ldots, n$. The ed_{ij} is the directed edge, from node i to node j, of digraph G. The adjacency elements of an edge ed_{ji} are positive, i.e., $a_{ij} > 0$ if and only if $ed_{ji} \in E$. A digraph is undirected if $a_{ij} = a_{ji}$ for $\forall i,j \in \{1,2,\ldots,n\}$.

A group of agents represents the nodes in a digraph G and unidirectional information exchange links among agents correspond to edges of the graph. An interaction topology among the battery agents shows the communication pattern at some particular time and is designed by using the digraph G. In adjacency matrix $\boldsymbol{A}$, an element a_{ij} is greater than zero, if and only if node i gets information from node j. A directed tree is defined as a directed graph in which every node except the root has exactly one parent. A directed (rooted) spanning tree of the digraph G is a subgraph such that this subgraph is a directed tree and consists of all the nodes of G. A spanning tree of G consists of n nodes and $n - 1$ edges and a path exists from root node to every other node. Thus, root node can send information to every other node.

The $n \times n$ Laplacian matrix $\boldsymbol{L_n} = (l_{ij})$, associated with the adjacency matrix $\boldsymbol{A}$ of a digraph G, is defined as given below:

$$l_{ij} = -a_{ij}, i \neq j \quad \text{and} \quad l_{ii} = \sum\nolimits_{j=1,j\neq i}^{n} a_{ij}$$

According to the definition of $\boldsymbol{L_n}$, it is ensured that in any row, $\sum_{j=1}^{n} l_{ij} = 0$, and it is the asymmetric matrix of a digraph. There is an aim to control all the nodes such that information state of all agents of a group converges to one single state [40–42].

In the uncertain power distribution system, the objectives are to develop a robust optimal distributed control protocol such that the battery agents of respective BESSs

should communicate to achieve the consensus for abovementioned goals during charging and discharging cycles and, furthermore, find global stability in the overall dynamic system. The control objective is to cater the imbalance in active power and uncertainty in the power distribution system with different BESSs and transforms this imbalance into the design of distributed control scheme. Two leader-follower pinning control schemes are designed for distributed control of the BESS to achieve their fair participations. These battery agents decide and control the power exchange to and from the respective BESSs. These agents exist at the BESS installation. These agents can receive information from the virtual leader to be pinned and to start distributed consensus control while communicating with neighboring battery agents, locally.

13.3 Robust Optimal Control

Briefly, the basics of robust optimal control are given as follows. Let the linear uncertain system be

$$x(k+1) = Ax(k) + Bu(k) + Ew(k) \tag{13.1}$$

where $x(k) \in R^n$ and $u(k) \in R^m$ are the state and input vectors, respectively. The sets X and U are polytopes, and $w(k)$ is the additive uncertainty present in the system. The Eq. (13.1) may be subject to constraints

$$x(k) \in X, \quad u(k) \in U \tag{13.2}$$

Now define the cost function for the given uncertainty $w \in W$ and the $u(k) \in U$.

$$J_w(k) = q(x(k), u(k)) \tag{13.3}$$

$$q(x(k), u(k)) = x^T Q x + u^T R u \tag{13.4}$$

The cost $J_w(k)$ is evaluated for the given uncertainty $w(k)$ and input $u(k)$ and with Eq. (13.1).

In case the probability density function is considered for the uncertainty $w(k)$ then

$$\text{Probability}\,[w(k) \in W] = 1 = \int_{w \in W} f(w)dw \tag{13.5}$$

The expected value of a function $g(w)$ of the uncertainty is defined as

$$E_w[g(w)] = \int_{w \in W} g(w)f(w)dw \tag{13.6}$$

The expected cost with admissible uncertainty is given as

$$J_w = E_w\left[x^T Q x + u^T R u\right] \tag{13.7}$$

$$\text{where} \begin{cases} x(k+1) = Ax(k) + Bu(k) + Ew(k) \\ x(k) \in X, \quad u(k) \in U \end{cases} \tag{13.8}$$

Now, the worst-case cost is defined as given below:

$$J_w = \max_w\left[x^T Q x + u^T R u\right] \tag{13.9}$$

$$\text{where} \begin{cases} x(k+1) = Ax(k) + Bu(k) + Ew(k) \\ x(k) \in X, \quad u(k) \in U \end{cases} \tag{13.10}$$

In all cases, the robust optimal control is given below while minimizing the cost function:

$$J_w^* = \min_u J_w \tag{13.11}$$

$$\text{where} \begin{cases} x(k+1) = Ax(k) + Bu(k) + Ew(k) \\ x(k) \in X, \quad u(k) \in U \end{cases} \tag{13.12}$$

13.4 BES System Modeling

The different scattered battery energy storage (BES) systems are considered to be connected to an AC system using bidirectional AC/DC converters. In this power distribution system, the BES systems are assumed to achieve reliable operation, in real time, at the distribution substation [15]. As the demand changes, the BES systems come into action. During off-peak hours, these systems can be charged, and in peak hours, these can be discharged. Therefore, the BES system can operate as a load during charging and as generator during discharging. Controlling and managing scattered BES systems with different ratings is a challenging task. The charging and discharging of a BES unit can be expressed as follows:

$$E_{es}(k+1) = E_{es}(k) - \frac{P_{es}(k)}{\eta_d}\Delta t, \text{ for } P_{es} > 0 \tag{13.13}$$

$$E_{es}(k+1) = E_{es}(k) - \eta_c P_{es}(k)\Delta t, \text{ for } P_{es} < 0 \tag{13.14}$$

where E_{es} is the stored energy in BES system, P_{es} is the power to be exchanged by BES system during charging and discharging, Δt is the time duration of k. η_d, and η_c are the discharging and charging efficiencies of BES system, respectively. The upper and lower limits of stored energy are as given below:

$$E_{es}^{\min} < E_{es}(k) < E_{es}^{\max} \tag{13.15}$$

where $E_{es}^{\max}$ and $E_{es}^{\min}$ are, respectively, the maximum and minimum bounds of the energy in the BES system.

The Eqs. (13.13) and (13.14) for BES system are modified as below:

$$\frac{E_{es}(k+1)}{E_{mm}} = \frac{E_{es}(k)}{E_{mm}} - \frac{P_{es}(k)}{E_{mm} \cdot \eta_d} \Delta t, \text{ for } P_{es} > 0 \tag{13.16}$$

$$\frac{E_{es}(k+1)}{E_{mm}} = \frac{E_{es}(k)}{E_{mm}} - \eta_c \frac{P_{es}(k)}{E_{mm}} \Delta t, \text{ for } P_{es} < 0 \tag{13.17}$$

where $E_{mm} = E_{es}^{\max} - E_{es}^{\min}$.

The power balance equation in an AC system at a time instant k

$$P_{grid}(k) + P_{ren}(k) + P_{es}(k) = P_{dem}(k) \tag{13.18}$$

where P_{grid} is grid supply, P_{ren} is the renewable power generation, P_{es} is power exchange by BES unit, and P_{dem} is the electrical demand.

The power balance equation incorporating uncertainties present in renewable power generation and electrical demand while dropping k for simplicity.

$$P_{grid} + (P_{ren} + \Delta P_{ren}) + (P_{es} + \Delta P_{es}) = (P_{dem} + \Delta P_{dem}) \tag{13.19}$$

where ΔP_{ren} and ΔP_{dem} represent uncertain parts of renewable power generation and electrical demand, respectively. The ΔP_{es} is the power exchange by BES unit to cater the uncertainties in an AC power distribution system.

On considering uncertainties in the system, the Eqs. (13.13) and (13.14) are modified as given below:

$$\begin{aligned} &\frac{E_{es}(k+1) + \Delta E_{es}(k+1)}{E_{mm}} = \frac{E_{es}(k) + \Delta E_{es}(k)}{E_{mm}} \\ &- \frac{P_{es}(k) + \Delta P_{es}(k)}{E_{mm} \cdot \eta_d} \Delta t, \text{ for } P_{es} > 0 \end{aligned} \tag{13.20}$$

$$\begin{aligned} &\frac{E_{es}(k+1) + \Delta E_{es}(k+1)}{E_{mm}} = \frac{E_{es}(k) + \Delta E_{es}(k)}{E_{mm}} \\ &- \eta_c \frac{P_{es}(k) + \Delta P_{es}(k)}{E_{mm}} \Delta t, \text{ for } P_{es} < 0 \end{aligned} \tag{13.21}$$

where ΔE_{es} represents the uncertain part of E_{es} .

For expected uncertainty, the (13.20) and (13.21) are modified as

$$\frac{E_{es}(k+1)+E\Delta E_{es}(k+1)}{E_{mm}}=\frac{E_{es}(k)+E\Delta E_{es}(k)}{E_{mm}} -\frac{P_{es}(k)+E\Delta P_{es}(k)}{E_{mm}\cdot\eta_d}\Delta t,\ \text{for } P_{es}>0 \tag{13.22a}$$

$$\frac{E_{es}(k+1)+E\Delta E_{es}(k+1)}{E_{mm}}=\frac{E_{es}(k)+E\Delta E_{es}(k)}{E_{mm}} -\eta_c\frac{P_{es}(k)+E\Delta P_{es}(k)}{E_{mm}}\Delta t,\ \text{for } P_{es}<0 \tag{13.23a}$$

For worst-case uncertainty, the (13.20) and (13.21) are modified as

$$\frac{E_{es}(k+1)+\max\limits_{\Delta E_{es}(k+1)}f(\Delta E_{es}(k+1))}{E_{mm}}=\frac{E_{es}(k)+\max\limits_{\Delta E_{es}(k)}f(\Delta E_{es}(k))}{E_{mm}} -\frac{P_{es}(k)+\max\limits_{\Delta P_{es}(k)}f(\Delta P_{es}(k))}{E_{mm}\cdot\eta_d}\Delta t,\ \text{for } P_{es}>0 \tag{13.22b}$$

$$\frac{E_{es}(k+1)+\max\limits_{\Delta E_{es}(k+1)}f(\Delta E_{es}(k+1))}{E_{mm}}=\frac{E_{es}(k)+\max\limits_{\Delta E_{es}(k)}f(\Delta E_{es}(k))}{E_{mm}} -\eta_c\frac{P_{es}(k)+\max\limits_{\Delta P_{es}(k)}f(\Delta P_{es}(k))}{E_{mm}}\Delta t,\ \text{for } P_{es}<0 \tag{13.23b}$$

On consideration of many BES systems, the aforementioned equations are generalized and used for *i*th BES system. Hence, the simplified model of *i*th BES system is

$$\begin{aligned}&x_i(k+1)=A_{x,i}x_i(k)+B_{x,i}u_i \text{ where } x_i=E_{i,es}/E_{i,mm},\\&u_i=P_{i,es}, A_{x,i}=1, B_{x,i}=\Delta t/\left(E_{i,mm}\cdot\eta_{i,d}\right) \text{ for } P_{i,es}>0,\\&B_{x,i}=\left(\eta_{i,c}\cdot\Delta t\right)/E_{i,mm} \text{ for } P_{i,es}<0\end{aligned} \tag{13.24}$$

The model pertaining to uncertainty

$$\begin{aligned}&y_i(k+1)=A_{y,i}y_i(k)+B_{y,i}v_i \text{where } y_i=\Delta E_{i,es}/E_{i,mm},\\&v_i=\Delta P_{i,es}, A_{y,i}=1, B_{y,i}=\Delta t/\left(E_{i,mm}\cdot\eta_{i,d}\right)\\&\text{for } P_{i,es}>0, B_{y,i}=\left(\eta_{i,c}\cdot\Delta t\right)/E_{i,mm} \text{for } P_{i,es}<0\end{aligned} \tag{13.25}$$

The abovementioned Eqs. (13.24) and (13.25) form the basis for development of the multi-agent system.

13.5 Agent-Based Robust Optimal Control Scheme

The multi-agent-based system deals with two control schemes which are optimal and incorporate uncertainties. Two leader-follower control schemes are given below.

$$x_i(k+1) = A_{x,i}x_i(k) + B_{x,i}u_i(k) \tag{13.26}$$

And

$$y_i(k+1) = A_{y,i}y_i(k) + B_{y,i}v_i(k) \tag{13.27}$$

$i = 1,\ldots,n$ where n is number of agents. The x_0,y_0 are the variables associated with leader agents. The abovementioned leader-follower schemes get consensus on following conditions:

$$x_i \to x_0 \text{ and } y_i \to y_0 \tag{13.28}$$

The linear consensus protocols are defined as given below:

$$u_i(k) = \sum_{j=1, j\neq i}^{n} a_{ij}\left[x_j(k) - x_i(k)\right] - b_i[x_i(k) - x_0] \tag{13.29}$$

And

$$v_i(k) = \sum_{j=1, j\neq i}^{n} w_{ij}\left[y_j(k) - y_i(k)\right] - d_i[y_i(k) - y_0] \tag{13.30}$$

The optimal control problem for the system (13.26)

$$\begin{aligned} &\min_{U(k)} J_x(U(k), X(0)) \\ &\text{subject to (13.26) and (13.28)} \end{aligned} \tag{13.31}$$

where

$$J_x(U(k), X(0)) = \sum_{k=0}^{\infty}\sum_{i=1}^{n} q_{x,i}(x_i - x_0)^2 + r_{x,i}u^2 \tag{13.32}$$

Similarly, the robust optimal control problem for the system (13.26) with expected cost function

$$\begin{aligned} &\min_{V(k)} \; EJ_y(V(k), Y(0)) \\ &\text{subject to (13.27) and (13.28)} \end{aligned} \tag{13.33}$$

where

$$E_{\Delta E(k)} J_y(V(k), Y(0)) = \sum_{k=0}^{\infty} \sum_{i=1}^{n} q_{y,i}(y_i - Ey_0)^2 + r_{y,i} v^2 \tag{13.34}$$

where $q_x > 0$, $q_y > 0$, $r_x > 0$, $r_y > 0$ and Ey_0 is the expected value of y_0.

Similarly, the robust optimal control problem for the system (13.26) with worst-case cost function

$$\begin{aligned} &\min_{V(k)} \; J_y(V(k), Y(0)) \text{ where} \\ &\text{subject to (13.27) and (13.28)} \end{aligned} \tag{13.35}$$

where

$$J_y(V(k), Y(0)) = \max_{\Delta E(k)} \sum_{k=0}^{\infty} \sum_{i=1}^{n} q_{y,i}(y_i - wy_0)^2 + r_{y,i} v^2 \tag{13.36}$$

where $q_x > 0$, $q_y > 0$, $r_x > 0$, $r_y > 0$, and wy_0 is the worst-case value of y_0.

Theorem For the joint optimal control problem, the optimal topology is star topology in which the follower i is only connected to the leader with the control gains $d_{x,i} = \frac{B_{x,0}}{2}\left(\frac{q_i}{r_i}\right)$ and $d_{y,i} = \frac{B_{y,0}}{2}\left(\frac{q_i}{r_i}\right)$ with the following assumptions:

Assumption 1:

$B_{x,1} = B_{x,2} = \ldots = B_{x,n} = B_{x,0}$ and $B_{y,1} = B_{y,2} = \ldots = B_{y,n} = B_{y,0}$

Assumption 2:

Let $B_{x,0} = \frac{2}{\sqrt{3}}\sqrt{\frac{r_i}{q_i}}$ and $B_{y,0} = \frac{2}{\sqrt{3}}\sqrt{\frac{r_i}{q_i}}$

The proof of this theorem is given in appendix.

13.5.1 Generation of x_0 and y_0

The x_0 is the desired value for all x_i and this value is provided to all agents from the leader agent. The leader agent knows the expected and worst case that may be associated with y_i, $i = 1,\ldots,n$, and y_0 is set to this expected and worst case. In

consensus-based robust optimal control scheme, all y_i track to this Ey_0 and wy_0, which are set to expected or worst-case value, respectively, as given below.

For expected value,

$$Ey_0 = f_e(\Delta E) \tag{13.37}$$

where f_e is the probability density function (pdf). Let, for any pdf,

$$Ey_0 = f_e(\Delta E) = \mathrm{G}_E g_E \leq p_E \tag{13.38}$$

where $\mathrm{G_E}$ and $\mathrm{g_E}$ are two different values which satisfy (13.37), and $\mathrm{p_E}$ is fixed constant value.

In worst case

$$wy_0 = \max_{\Delta E} y_i, \quad \forall i \in [1, \ldots, n] \tag{13.39}$$

Let, on maximizing the worst case

$$wy_0 = \max_{\Delta E} y_i = G_w g_w \leq p_w, \quad \forall i \in [1, \ldots, n] \tag{13.40}$$

Similar to (13.37), $\mathrm{G_w}$ and $\mathrm{g_w}$ are two different values which satisfy (13.39), and $\mathrm{p_w}$ is fixed constant value. The ($\mathrm{p_E}$,$\mathrm{G_E}$, $\mathrm{g_E}$) and ($\mathrm{p_w}$,$\mathrm{G_w}$, $\mathrm{g_w}$) are identified and set to the values based on past data.

With the allowed uncertainty in the system, the Eq. (13.34) is rewritten as

$$E_{\Delta E(k)} J_y(V(k), Y(0)) = \sum_{k=0}^{\infty} \sum_{i=1}^{n} q_{y,i} (y_i - p_E)^2 + r_{y,i} v^2 \tag{13.41}$$

$$E_{\Delta E(k)} J_y(V(k), Y(0)) = \sum_{k=0}^{\infty} \sum_{i=1}^{n} q_{y,i} (e_E)^2 + r_{y,i} v^2 \tag{13.42}$$

where $e_E = (y_i - p_E)$.

Similarly, on maximizing the worst case in the uncertainty, the equation is modified as

$$J_y(V(k), Y(0)) = \sum_{k=0}^{\infty} \sum_{i=1}^{n} q_{y,i} (y_i - p_w)^2 + r_{y,i} v^2 \tag{13.43}$$

$$J_y(V(k), Y(0)) = \sum_{k=0}^{\infty} \sum_{i=1}^{n} q_{y,i} (e_w)^2 + r_{y,i} v^2 \tag{13.44}$$

where $e_w = (y_i - p_w)$.

13.6 Results and Discussions

The test microgrid is shown in the Fig. 13.1. The sizes of the battery energy storage devices are 0.2 MW/0.8MWh, 0.15 MW/0.75MWh, 0.1 MW/0.4MWh, 0.15 MW/0.45MWh, and 0.4 MW/1.6MWh with charging and discharging efficiencies $\eta_c = \eta_d = 80\%$, and the size of solar PV system is 1MWp. The maximum and minimum allowed energy on energy storage devices are $Emax_1 = 0.8MWh$ and $Emin_1 = 0.35MWh$, $Emax_2 = 0.75MWh$ and $Emin_2 = 0.40MWh$, $Emax_3 = 0.4MWh$ and $Emin_3 = 0.1MWh$, $Emax_4 = 0.45MWh$ and $Emin_4 = 0.1MWh$, and $Emax_5 = 1.6MWh$ and $Emin_5 = 1.25MWh$, respectively. In order to satisfy assumptions 1 and 2, the discharging efficiencies of these energy storage devices are assumed as 0.70, 0.85, 0.95, 0.82, and 0.85, and charging efficiencies are assumed as 0.86, 0.89, 0.91, 0.89, and 0.89, respectively.

The considered load profile of electrical demand and solar PV generation profile with added uncertainty are shown in Figs. 13.2 and 13.3, respectively. The included uncertainty remains within the permissible range as per Eqs. (13.38) and (13.40). The optimal energy and power are shared based on given power generation and electrical demand as shown in Figs. 13.4, 13.5, and shared optimal uncertain energy and power are shown in 13.6, and 13.7, respectively. Assume $q_i = r_i = 1$ for $i = 1,...,5$ then $d_{x,i} = d_{y,i} = 1.73$.

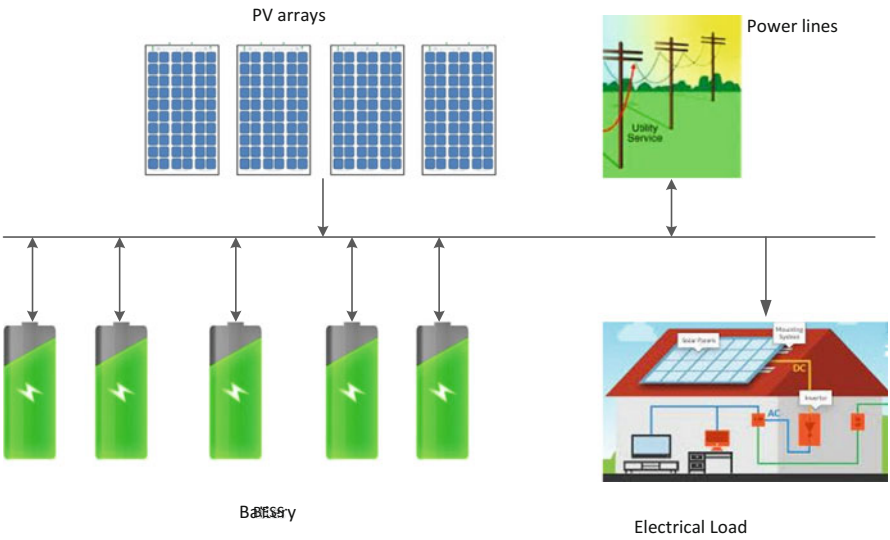

Fig. 13.1 Test microgrid

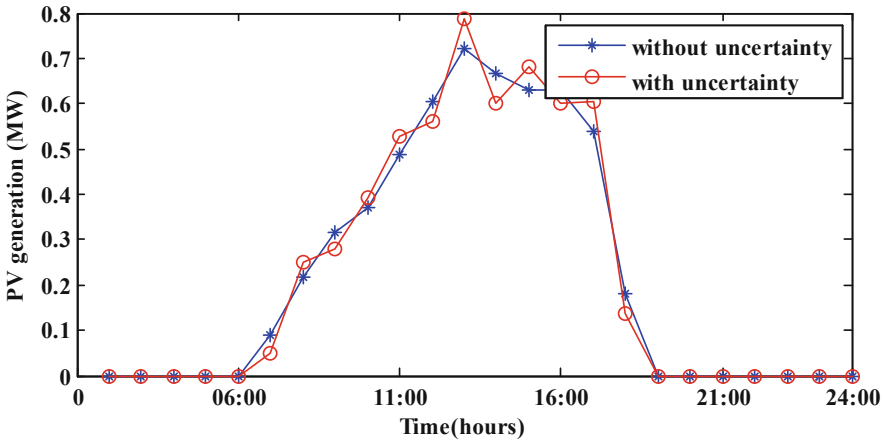

Fig. 13.2 Forecasted PV generation (blue) and PV generation with uncertainty (red)

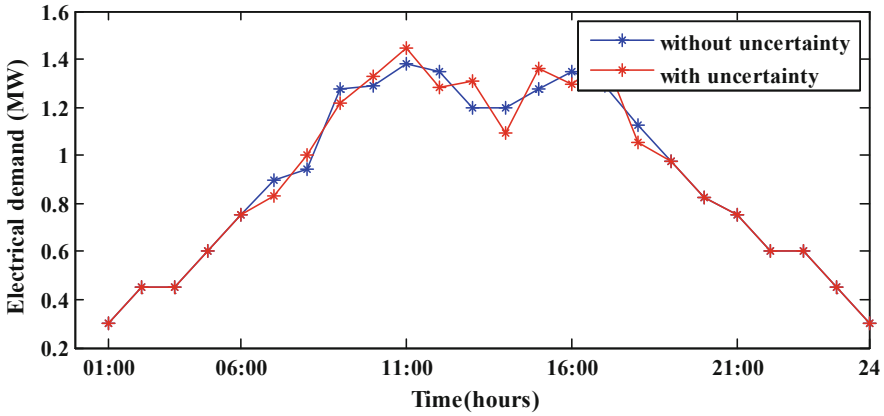

Fig. 13.3 Electrical demand

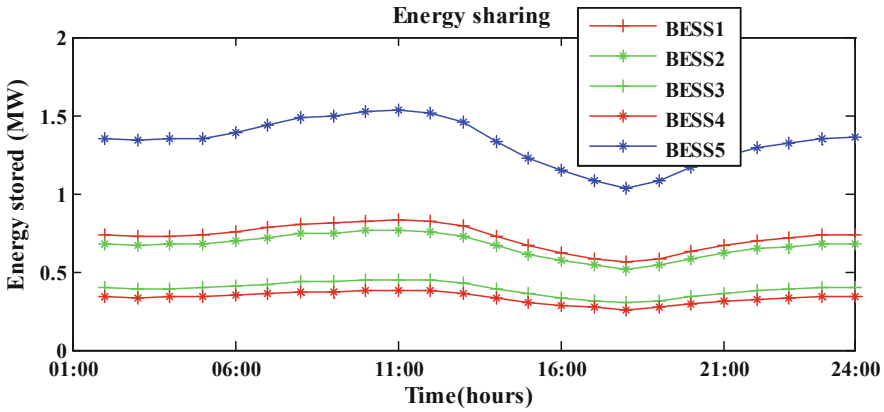

Fig. 13.4 Energy stored shared by different BESSs

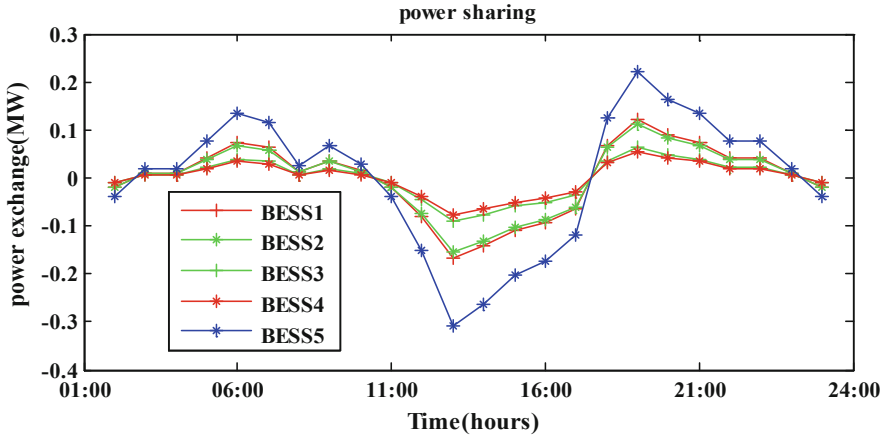

Fig. 13.5 Power exchange shared by different BESSs

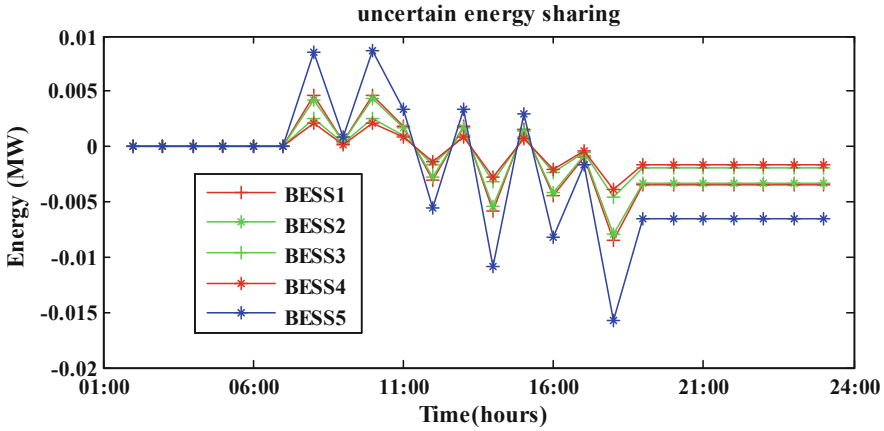

Fig. 13.6 Uncertain energy shared by different BESSs

13.7 Conclusions

This chapter has discussed agent-based distributed robust optimal control scheme. This scheme considers two objective functions out of which second objective function pertains to the uncertainties which are present in the power distribution system integrated with renewable power generation along with energy storage devices. Distributed multi-agent system works for deciding the charging and discharging of the batteries in the presence of uncertainties. In two expected and worst cases, all the agents get consensus and be driven to the values decided by the leader agent. In this distributed robust optimal control scheme, the optimal topology for communication is the star topology as proved in the theorem.

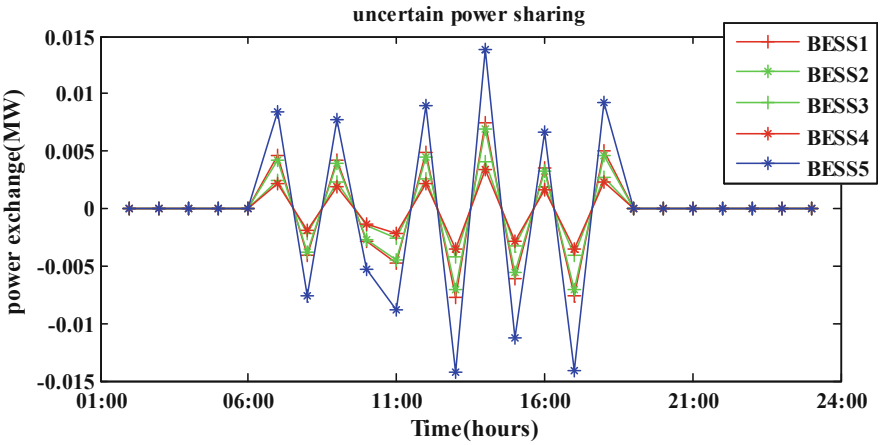

Fig. 13.7 Uncertain power exchange shared by different BESSs

Appendix

Proof of theorem

Let the error system for (13.26) be

$$\begin{aligned} e(k+1) &= A_x e(k) + B_x U(k), \\ U(k) &= -L_x e(k) \end{aligned} \tag{13.45}$$

where $A_x = \ diag\ (A_{x,1}, A_{x,2}, \ldots, A_{x,n})$ and $B_x = \ diag\ (B_{x,1}, B_{x,2}, \ldots, B_{x,n})$ and

$$e(k) = X(k) - 1_n \otimes U(k) \tag{13.46}$$

The modified LQR-based optimal control problem is

$$\min_{U(k)} \sum_{k=0}^{\infty} e(k)^T Q e(k) + U(k)^T R U(k) \tag{13.47}$$

For the system $X(k+1) = AX(k)+BU(k)$, the discrete time ARE is

$$A^T PA - P + Q - A^T PB\left(R + B^T PB\right)^{-1} B^T PA = 0 \tag{13.48}$$

For the system (13.45), the ARE is

$$Q = PB_x\left(R + B_x^2 P\right)^{-1} B_x P \tag{13.49}$$

where $A = A_x = 1$ and $B = B_x$.

Let $B_{x,1} = B_{x,2} = \ldots = B_{x,n} = B_{x,0}$

Then matrix $B_x = B_{x,0} I_n$

The optimal feedback gain matrix is

$$L_x = \left(R + B_{x,0}^2 I_n P\right)^{-1} B_{x,0} I_n P \tag{13.50}$$

Multiply R^{-1} both sides of (13.49) then

$$R^{-1}Q = R^{-1} P B_{x,0} I_n \left(R + B_{x,0}^2 I_n P\right)^{-1} B_{x,0} I_n P \tag{13.51}$$

$$R^{-1}Q = R^{-1} P B_{x,0} \left(I_n + B_{x,0}^2 R^{-1} P\right)^{-1} B_{x,0} R^{-1} P \tag{13.52}$$

Since it is known that

$$\left(I_n + B_{x,0}^2 R^{-1} P\right)^{-1} = I_n - B_{x,0}^2 R^{-1} P \left(I_n + B_{x,0}^2 R^{-1} P\right)^{-1} \tag{13.53}$$

We now get

$$\begin{aligned} &R^{-1} P B_{x,0} \left(I_n + B_{x,0}^2 R^{-1} P\right) B_{x,0} R^{-1} P = \left[B_{x,0} R^{-1} P\right]^2 - B_{x,0}^2 R^{-1} P \\ &\times \left[R^{-1} P B_{x,0} \left(I_n + B_{x,0}^2 R^{-1} P\right)^{-1} B_{x,0} R^{-1} P\right] \end{aligned} \tag{13.54}$$

$$R^{-1}Q = B_{x,0}^2 \left(R^{-1} P\right)^2 - B_{x,0}^2 R^{-1} P R^{-1} Q \tag{13.55}$$

On simplification it is obtained that

$$R^{-1}P = \frac{1}{2}\left[R^{-1}Q + \sqrt{\left(R^{-1}Q\right)^2 + \frac{4R^{-1}Q}{B_x^2}}\right] \tag{13.56}$$

Hence, the optimal feedback gain matrix is

$$L_x^* = \frac{B_{x,0}}{2}\left[\sqrt{\left(R^{-1}Q\right)^2 + \frac{4R^{-1}Q}{B_{x,0}^2}} - R^{-1}Q\right] \tag{13.57}$$

Let

$$L_x^* = diag(d_{x,1}, d_{x,2} \ldots, d_{x,n}) \tag{13.58}$$

Then, for *i*th agent the feedback gain is

$$d_{x,\mathrm{i}} = \frac{B_{x,0}}{2}\left[\sqrt{\left(\frac{q_i}{r_i}\right)^2 + \frac{4q_i}{B_{x,0}^2 r_i}} - \frac{q_i}{r_i}\right] \tag{13.59}$$

Similarly, it can be proved that

$$d_{y,\mathrm{i}} = \frac{B_{y,0}}{2}\left[\sqrt{\left(\frac{q_i}{r_i}\right)^2 + \frac{4q_i}{B_{y,0}^2 r_i}} - \frac{q_i}{r_i}\right] \tag{13.60}$$

Let

$$B_{x,0}^2 = \frac{4}{3}\frac{r_i}{q_i} \tag{13.61}$$

Then from (13.59)

$$d_{x,\mathrm{i}} = \frac{B_{x,0}}{2}\left[\sqrt{\left(\frac{q_i}{r_i}\right)^2 + 3\left(\frac{q_i}{r_i}\right)^2} - \frac{q_i}{r_i}\right] \tag{13.62}$$

$$d_{x,\mathrm{i}} = \frac{B_{x,0}}{2}\frac{q_i}{r_i} \tag{13.63}$$

Similarly, we can obtain

$$d_{y,\mathrm{i}} = \frac{B_{y,0}}{2}\frac{q_i}{r_i} \tag{13.64}$$

While

$$B_{y,0}^2 = \frac{4}{3}\frac{r_i}{q_i} \tag{13.65}$$

References

1. Sumathi, S., Kumar, L. A., & Surekha, P. (2015). *Solar PV and wind energy conversion systems an introduction to theory, modeling with MATLAB/SIMULINK, and the role of soft computing techniques*. Cham: Springer.
2. Song, S., Ko, B., Suh, J., Han, C., & Jang, G. (2017). Operation algorithm of PV/BESS application considering demand response uncertainty in an independent microgrid system. *Journal of International Council on Electrical Engineering, 7*(1), 242–248.
3. Prusty, B., Ali, S., & Sahoo, D. (2012). Modeling and control of grid connected hybrid photo voltaic/battery distributed generation system. *International Journal of Engineering Research and Technology, 24*(1), 125–132.
4. Rai, V., Reeves, C., & Margolis, R. (2016). Overcoming barriers and uncertainties in the adoption of residential solar PV. *Renewable Energy, 89*, 498–505.
5. Attarha, A., Amjady, N., & Dehghan, S. (2018). Affinely adjustable robust bidding strategy for a solar plant paired with a battery storage. *IEEE Transactions on Smart Grid, PP*(99), 1. https://doi.org/10.1109/TSG.2018.2806403.
6. Ela, E., Diakov, V., Ibanez, E., & Heaney, M. (2013). Impacts of variability and uncertainty in solar photovoltaic generation at multiple timescales. *National Renewable Energy Laboratory, 1*, 41.
7. de la Fuente, D. V., Rodriguez, C. L. T., Garcera, G., Figueres, E., & Gonzalez, R. O. (2013). Photovoltaic power system with battery backup with grid-connection and islanded operation capabilities. *IEEE Transactions on Industrial Electronics, 60*(4), 1571–1581.
8. Kim, S.-T., Bae, S., Kang, Y. C., & Park, J.-W. (2015). Energy management based on the photovoltaic hpcs with an energy storage device. *IEEE Transactions on Industrial Electronics, 62*(7), 4608–4617.
9. Atwa, Y. M., El-Saadany, E. F., Salama, M. M. A., & Seethapathy, R. (2010). Optimal renewable resources mix for distribution system energy loss minimization. *IEEE Transactions on Power Systems, 25*(1), 360–370.
10. Zeng, J., Liu, J. F., Wu, J., & Ngan, H. W. (2011). A multi-agent solution to energy management in hybrid renewable energy generation system. *Renewable Energy, 36*(5), 1352–1363.
11. Conti, S., & Raiti, S. (2007). Probabilistic load flow using Monte Carlo techniques for distribution networks with photovoltaic generators. *Solar Energy, 81*, 1473–1481.
12. Paparoditis, E., & Sapatinas, T. (2013). Short-term load forecasting: the similar shape functional time-series predictor. *IEEE Transactions on Power Systems, 28*(4), 3818–3825.
13. Xydas, E., Qadrdan, M., Marmaras, C., Cipcigan, L., Jenkins, N., & Ameli, H. (2017). Probabilistic wind power forecasting and its application in the scheduling of gas-fired generators. *Applied Energy, 192*, 382–394.
14. Sun, X., Luh, P. B., Michel, L. D., Corbo, S., Cheung, K. W., Guan, W., & Chung, K. (2013). An efficient approach for short-term substation load forecasting. *IEEE Power & Energy Society General Meeting*. https://doi.org/10.1109/PESMG.2013.6673009.
15. Hung, D. Q., Mithulananthan, N., & Bansal, R. C. (2014). Integration of PV and BES units in commercial distribution systems considering energy loss and voltage stability. *Applied Energy, 113*, 1162–1170.
16. Murata, A., Ohtake, H., & Oozeki, T. (2018). Modeling of uncertainty of solar irradiance forecasts on numerical weather predictions with the estimation of multiple confidence intervals. *Renewable Energy, 117*, 193–201.
17. Wolfs, P., Emami, K., Lin, Y., & Palmer, E. (2018). Load forecasting for diurnal management of community battery systems. *Journal of Modern Power System and Clean Energy, 6*(2), 215–222.
18. Rahbari-Asr, N., Zhang, Y., & Mo-Yuen, C. (2015). Consensus-based distributed scheduling for cooperative operation of distributed energy resources and storage devices in smart grids. *IET Generation, Transmission and Distribution, 10*(5), 1268–1277.

19. Zhao, T., & Ding, Z. (2018). Distributed agent consensus-based optimal resource management for microgrids. *IEEE Transactions on Sustainable Energy, 9*(1), 443–452.
20. Fortenbacher, P., Mathieu, J. L., & Andersson, G. (2017). Modeling and optimal operation of distributed battery storage in low voltage grids. *IEEE Transactions on Power Systems, 32*(6), 4340–4350.
21. Xu, Y. (2015). Optimal distributed charging rate control of plug-in electric vehicles for demand management. *IEEE Transactions on Power Systems, 30*(3), 1536–1545.
22. Xu, Y., Yang, Z., Gu, W., Li, M., & Deng, Z. (2017). Robust real-time distributed optimal control based energy management in a smart grid. *IEEE Transactions on Smart Grid, 8*(4), 1568–1579.
23. Morstyn, T., Hredzak, B., & Agelidis, V. G. (2018). Network topology independent multi-agent dynamic optimal power flow for microgrids with distributed energy storage systems. *IEEE Transactions on Smart Grid, 9*(4), 3419–3429.
24. Dimeas, A. L., & Hatziargyrious, N. D. (2005). Operation of multi agent system for micro grid control. *IEEE Transaction Power System, 20*(3), 1447–1445.
25. Dimeas, A. L., & Hatziargyriou, N. D. (2007, November). *Agent based control of virtual power plants*. Interference conference on intelligent systems applications to power systems. ISAP 2007, Toki Messe, Niigata.
26. McArthur, S. D. J., Davidson, E. M., Catterson, M. V., Dimeas, A. L., Ponci, F., Hatziargyriou, N. D., & Funabashi, T. (2007). Multi agent systems for power engineering applications –part I: Concepts, approaches and technical challenges. *IEEE Transaction on Power Systems, 22*(4), 1743–1752.
27. McArthur, S. D. J., Davidson, E. M., Catterson, V. M., Dimeas, A. L., Ponci, F., Hatziargyriou, N. D., & Funabashi, T. (2007). Multi agent systems for power engineering applications –part II: Technologies, standards and tools for building multi agent systems. *IEEE Transaction on Power Systems, 22*(4), 1753–1759.
28. Colson, C. M., Nehrir, M. H., & Gunderson, R. W. (2011, August–September). *Multi agent microgrid power management*. 18th IFAC World Congress, Milano.
29. Fakham, H., Doniec, A., Colas, F., & Guillaud, X. (2010). *A multi-agent system for a distributed power management of micro turbine generators connected to grid*. *IFAC Proceedings. 43*(1), 175–180.
30. Davidson, E. M., McArthur, S. D. J., McDonald, J. R., Cumming, T., & Watt, I. (2006). Applying multi-agent system technology in practice: Automated management and analysis of SCADA and digital fault recorder data. *IEEE Transaction on Power Systems, 21*(2), 559–566.
31. Huang, K., Srivastava, S. K., Cartes, D. A., & Sun, L. (2009). Market based multi-agent system for reconfiguration of shipboard power systems. *Electric Power Systems, 79*, 550–556.
32. Praca, I., Ramos, C., Vale, Z., & Corderio, M. (2003). MASCEM: A multi agent system that simulates competitive electricity markets. *IEEE Intelligent System, 18*(6), 54–60.
33. Karitov, V. S. (2004). Real-world market representation with agents. *IEEE Power Energy Magazine, 2*(4), 39–46.
34. Nagata, T., & Sasaki, H. (2002). A multi-agent approach to power system restoration. *IEEE Transaction Power System, 17*(2), 457–462.
35. McArthur, S. D. J., Strachan, S. M., & Jahn, G. (2004). The design of a multi-agent transformer condition monitoring system. *IEEE Transaction Power System, 19*(4), 1845–1852.
36. Mangina, E. E., McArthur, S. D. J., McDonald, J. R., & Moyes, A. (2001). A multi agent system for monitoring industrial gas turbine start-up sequences. *IEEE Transaction Power System, 16* (3), 396–401.
37. Buse, D. P., Sun, P., Wu, Q. H., & Fitch, J. (2003, March–April). Agent – Based substation automation. *IEEE Power Energy Magazine, 1*(2), 50–55.
38. Logenthiran, T., Srinivasan, D., & Khambadkone, A. M. (2011). Multi-agent system for energy resource scheduling of integrated microgrids in a distributed system. *Electrical Power System Research, 81*, 138–148.

39. Hossack, J., Menal, A. J., McArthur, S. D. J., & McDonald, J. R. (2003). A multi-agent architecture for protection engineering diagnostic assistance. *IEEE Transaction on Power System, 18*(2), 639–647.
40. Fax, J. A., & Murray, R. M. (2004). Information flow and cooperative control of vehicle formations. *IEEE Transactions Automatic Control, 49*, 1464–1476.
41. Reza, O.-S., Fax, J. A., & Murray, R. M. (2007). Consensus and cooperation in networked multi-agent systems. *Proceedings of the IEEE, 95*(1), 215–233.
42. Ren, W., & Beard, R. W. (2008). *Distributed consensus in multi-vehicle cooperative control: Theory and applications*. London: Springer.